P H Y S I C A L R E V I E W L E T T E R S

Room-Temperature Polariton Lasing in Semiconductor Microcavities

S. Christopoulos, G. Baldassarri Höger von Högersthal, A. J. D. Grundy,
P. G. Lagoudakis, A. V. Kavokin, and J. J. Baumberg*

School of Physics and Astronomy, University of Southampton, Highfield, Southampton, SO17 1BJ, United Kingdom

G. Christmann, R. Butté, E. Feltin, J.-F. Carlin, and N. Grandjean

École Polytechnique Fédérale de Lausanne (EPFL), Institute of Quantum Electronics and Photonics, 1015 Lausanne, Switzerland

We observe a room-temperature low-threshold transition to a coherent polariton state in bulk GaN microcavities in the strong-coupling regime. Nonresonant pulsed optical pumping produces rapid thermalization and yields a clear emission threshold of 1 mW, corresponding to an absorbed energy density of 29 μJ cm^{-2}, 1 order of magnitude smaller than the best optically pumped (In,Ga)N quantum-well surface-emitting lasers (VCSELs). Angular and spectrally resolved luminescence show that the polariton emission is beamed in the normal direction with an angular width of $\pm 5°$ and spatial size around 5 μm.

Microcavity (MC) emitters possess exceptional optical properties by virtue of their small size. When one or more dimensions of the cavity are on the order of the wavelength of confined light a host of new effects arise, including low-threshold lasing, directionally beamed luminescence, high speed modulation, and enhanced nonlinear conversion. Microcavities containing media that couple strongly to light can enter a regime of strong coupling which produces new admixed quasiparticles, the polaritons, which are half light and half matter and possess unusual dispersion relations [1]. In semiconductor microcavities, recent discoveries have shown that these polaritons differ completely from excitons in their enormous nonlinear scattering cross sections [2,3] and their bosonic statistics. This can lead to polariton lasing, the spontaneous emission of coherent light by condensates of exciton-polaritons [4–8]. Unlike conventional lasers, polariton lasers have no threshold condition linked to the inversion of the population. However, these phenomena exist only at cryogenic temperatures, limited by the small energy splitting of polaritons below the excitons. Recent work on CdTe quantum-well (QW) semiconductor microcavities has been promising, with polariton emission showing a distinct threshold to a coherent condensate state as the nonresonant excitation is increased. However, these phenomena are destroyed by thermal decoherence for temperatures above 220 K [9,10].

Here we show for the first time coherent polariton emission at room temperature from bulk GaN microcavities in the strong-coupling regime. We show that luminescence from the most strongly coupled lower polariton branch exhibits a transition with a clear threshold to a coherent state which is localized in a few micron sized regions of the excited sample. Polariton luminescence narrows to a forward directed cone, with a narrow spectral linewidth. Such GaN microcavities open up a host of technological possibilities including low-threshold emitters, nonlinear

optical elements and amplifiers, and quantum correlated sources.

The viability of nitride-based microcavities has been a compelling goal over the last few years, due to the large oscillator strength in these materials as well as their large exciton-binding energy suggesting potential high-temperature performance [6]. Recent reports have confirmed that Rabi splittings between upper (UP) and lower (LP) polariton branches can exceed 50 meV, an order of magnitude larger than comparable III-V based microcavities [11,12]. While the introduction of QWs generally optimizes light-matter coupling in III-V microcavities (due to the greater exciton-binding energy and better QW overlap with the cavity standing wave), the nitride-based QWs currently exhibit broad linewidths and are plagued by the quantum-confined Stark effect [13]. Hence we use bulk GaN microcavities of a hybrid design [Fig. 1(a), inset]. The bulk $3\lambda/2$ GaN central spacer is sandwiched between a bottom 35 period $Al_{0.85}In_{0.15}N/Al_{0.2}Ga_{0.8}N$ distributed Bragg reflector (DBR) and a top 10 period dielectric SiO_2/Si_3N_4 DBR, as discussed in Ref. [12]. This choice of lower DBR is lattice matched, reducing the built-in tensile strain occurring during growth, preventing the formation of cracks and/or dislocations, and leading to a quality factor in excess of ~2800 in similar MC structures [14]. These large-area samples look transparent to the eye and are of high quality with few scattering defects. All measurements in this Letter are taken at room temperature.

Large-area reflectivity spectra of the sample at near-normal incidence [~5°, Fig. 1(a)] resolve the stop band of the top dielectric reflector, together with the weak lower polariton mode at 3.4 eV. The theoretical angular dispersion of the absorption within the GaN cavity is calculated using a transfer matrix formalism and the full dielectric constants [15], both without and with the resonant excitonic component [16] at 3.42 eV [Fig. 1(b) and 1(c)],
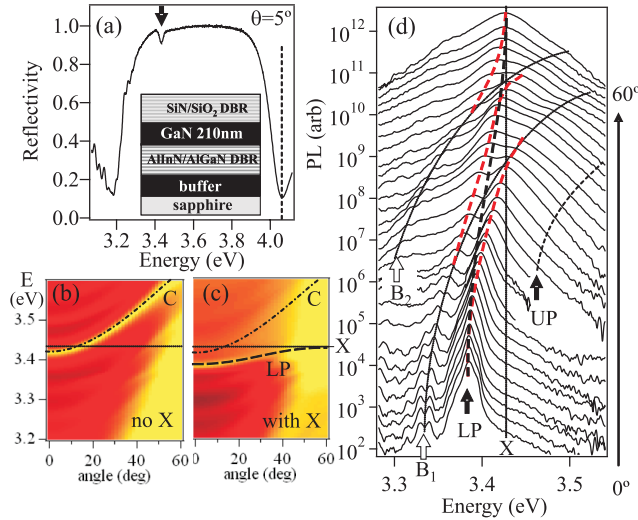
FIG. 1 (color online).   (a) Microcavity reflectivity at 300 K and $\theta \sim 5°$, with lower polariton mode marked (arrow). Dashed line shows nonresonant pump energy. Inset shows the layer structure. (b), (c) Theoretical angular dispersion both without (b) and with (c) the resonant exciton contribution to the GaN cavity (ω_{LP} dashed line, ω_{cav} dash-dotted line) for a slightly negatively detuned cavity ($\Delta = -10$ meV). (d) Angle-resolved PL at low powers up to 60°, with lower (LP) and upper (UP) polaritons, exciton (X), and Bragg modes (B) marked.

showing the effect of strong coupling for this bulk microcavity. The different average refractive indices of top and bottom DBRs lead to different in-plane dispersions and hence to their progressive detuning with angle. At high angles ($\theta > 50°$) the top DBR becomes essentially transparent allowing direct interrogation of the exciton distribution. The lower polariton dispersion is strongly flattened by the coupling, while the upper polariton in a bulk microcavity is broadened and almost completely attenuated by the exciton continuum at the same energy. In addition, Bragg modes on either side of the narrow stop band, lower GaN-based DBR, are visible which also cross the exciton dispersion [17].

In order to investigate the emission under nonresonant pumping of these bulk GaN microcavities, we constructed a UV femtosecond goniometer (similar to [2]) in which both incident pump and emission angles can be scanned up to 80°. A 150 fs spectrally tuneable pump pulse is produced by frequency doubling the visible output of a $f_p = 250$ kHz optical parametric amplifier. The p-polarized pulses are focused down to a 60 μm diameter spot on the dielectric top DBR (since the GaN buffer is opaque) to nonresonantly excite the sample, and the resulting luminescence is collected in a particular emission direction over an angular range of $\pm 3°$, and focused onto a UV multimode collection fibre coupled to a 0.5 m monochromator and liquid N_2-cooled CCD.

Initially the pump wavelength and angle are scanned systematically from 250–320 nm while monitoring the photoluminescence (PL) emerging at normal incidence.

This confirms that optimum pumping occurs in resonance with the first Bragg mode above the upper DBR stop band [dashed line Fig. 1(a)], and hence for the rest of the results here we pump at 20° and $\hbar\omega = 4.14$ eV. Unlike usual III-V microcavities, this sample is not wedged, but some tuning of the cavity mode around the exciton energy, $\Delta = \omega_c - \omega_x$, due to photonic disorder and sample thickness reduction close to the border is achieved by scanning around the sample. The characteristic results we observe are seen over a large area of the sample, although we note that the pump needs to be simultaneously retuned with the Bragg resonance. PL spectra at low power (10 W cm^{-2}) are recorded as a function of angle for a particular spot on the sample [Fig. 1(d)], with detuning $\Delta \sim -10$ meV. As in the theory, the lower polariton (black dashed line) is clearly visible increasing towards the exciton from below, but the upper polariton PL is very weak under these pumping conditions. Also visible are Bragg modes ($B_{1,2}$ dotted lines) resonant inside the lower DBR which also strongly couple to the GaN exciton, leading to additional anticrossings at high angles (red dashed line) [17]. Similar strong-coupling bulk GaN microcavity dispersions have been previously reported [11,12].

The integrated output intensity collected at normal incidence for these conditions is shown as a function of pump intensity in Fig. 2 with slightly positive detuning. A clear nonlinear behavior is found for the emission at $\lambda \simeq 365$ nm, with an increase of over 10^3 at the critical threshold around $I_{th} = 1.0$ mW. This corresponds to a density of $N_{3D} \sim 2.2 \times 10^{18}$ cm^{-3},[18] which is an order of magnitude below both the Mott density $\simeq 1 - 2 \times 10^{19}$ cm^{-3} in GaN at 300 K [19], and the transparency density for bulk GaN which provides the lower limit for lasing. This threshold density is nearly an order of magnitude below the smallest threshold density ever observed in (In,Ga)N QW VCSELs [20]. These features are similar to polariton lasing reported in II-VI and III-V microcavities at low temperature [7–9]. Analysis of the power dependence [Fig. 2(c)] yields the probability, $\beta \sim (7000)^{-1}$, that spontaneously emitted polaritons emerge in the mode which undergoes stimulated scattering [21,22]. In conventional microcavity lasers, the cavity volume is made small (photons confined in 3D) leading to a large Purcell factor which produces a β exceeding 1%. Planar semiconductor microcavities differ in that the cavity confines photons in only 1D, but the stimulated scattering from the bosonic nature of the polaritons leads to inversionless coherent emission (termed polariton lasing) unrelated to the transparency condition [6]. Instead, stimulated scattering takes off when the occupation in any polariton mode reaches unity, which defines the polariton laser threshold. From the emitted power (80 μW at 4 mW pump) and the 5° HWHM emission cone (discussed below), we estimate 10^6 polaritons/state/pulse above threshold [3], and hence estimated occupations of ≥ 10 at threshold [23].

Commensurate with the exponential power increase is a sudden collapse in emission linewidth at threshold
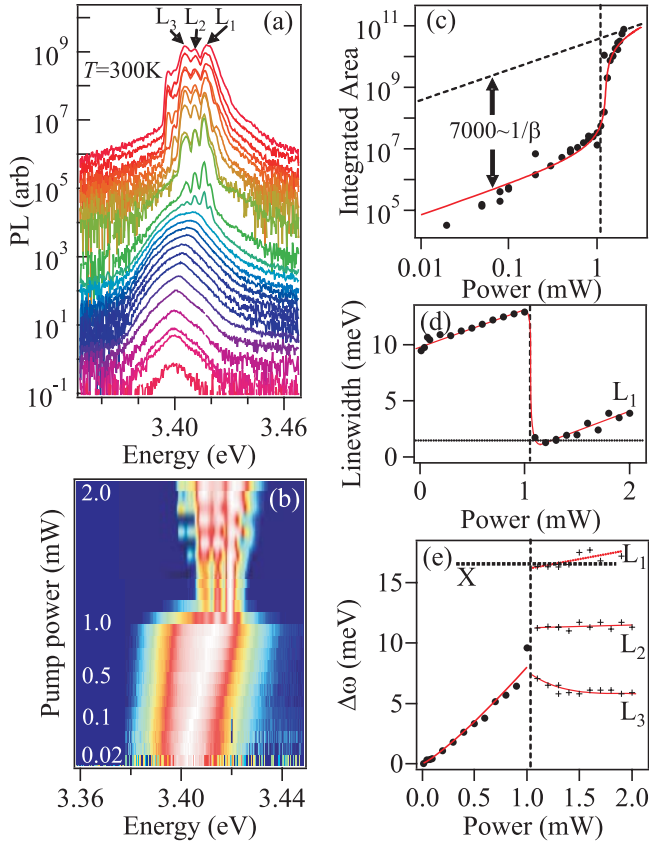
FIG. 2 (color online). (a), (b) Emission spectra at pump powers from 20 μW to 2 mW at 0°, shifted in (a) for clarity, (b) false color, log scale. (c) Integrated intensity vs pump power (solid points), with fit. (d) Spectral linewidth and (e) energy shift of peak emission with pump power (for different modes L_{1-3}).

[Fig. 2(d)] down to our resolution limit (1.7 meV). We find that the precise peak energy position is extremely sensitive to the spatial alignment on the sample. Spectra integrated over 10 ms often show multiple line emission [e.g., L_{1-3} in Fig. 2(a)] with the spacing between these sharp emission peaks being irregular, and varying over both time and sample position. As we discuss below, we speculate that photonic disorder localizes the polariton condensate laterally (similar to CdTe microcavities [9]), with the different modes first attaining unity occupation on different laser shots statistically. This behavior contrasts with previous observations of coexistence of strong coupling and low threshold lasing [24].

As the pump power increases, the peak emission energy *blueshifts* until it locks at threshold [Fig. 2(e)]. Such a behavior is expected from polariton-polariton interactions[25], with $\hbar\Delta\omega_{LP} = \frac{1}{2}\hbar\Delta\omega_X \sim 3.3\pi E_b a_B^3 N_{3D}$ at threshold, where $E_b = 28$ meV is the exciton-binding energy, $a_B = 3.5$ nm is the Bohr radius, and N_{3D} is the exciton density. From this relation we can again estimate $N_{3D} \sim 8 \times 10^{17}$ cm^{-3} at threshold, similar to that estimated directly above and confirming sub-Mott density coherent emission. We further note that the blueshifted emission is only seen around $k = 0$ and remains below

the exciton energy (marked X), while the excitons (directly observed at $\theta = 60°$) exhibit little power broadening but some heating $\Delta T < 100$ K in their Boltzmann-like high-energy tails. By contrast, incoherent GaN emission is known to *redshift* with increasing pump power [19], while thermal cavity expansion would have a similar effect and we measure no blueshift in a comparable empty microcavity.

Observation of a threshold is not a sufficiently stringent requirement to prove a coherent state. Hence we measure the spatial polariton distribution as a function of power (Fig. 3). Below threshold the spatial emission matches closely the pump spot [Fig. 3(a)], switching to typically $\Delta x = 5$ μm spots above threshold varying slightly with sample position [Fig. 3(b)]. This implies that only ~1% of the pumped spot is involved in the strong emission, thus suggesting efficiencies within this small area close to 100%. Further evidence is provided by measuring the first order coherence of the emission. We pass the emission through a Michelson interferometer and record the k-space images. Fringes are seen for time delays up to ~700 fs between the paths [Fig. 3(d)] matching the ultra-short emission lifetime [Fig. 4(b)].

In order to study the buildup of the emission and observe the collapse in k space, we perform angularly resolved detection for different incident pump powers without moving either sample or pump laser focus. The integrated intensities on each branch are extracted when pumping below, at, and above the threshold [Fig. 4(a)]. Similarly to our observation of a localization in real space, in k space we measure a reduction down to HWHM $\Delta\theta = 5°$ on
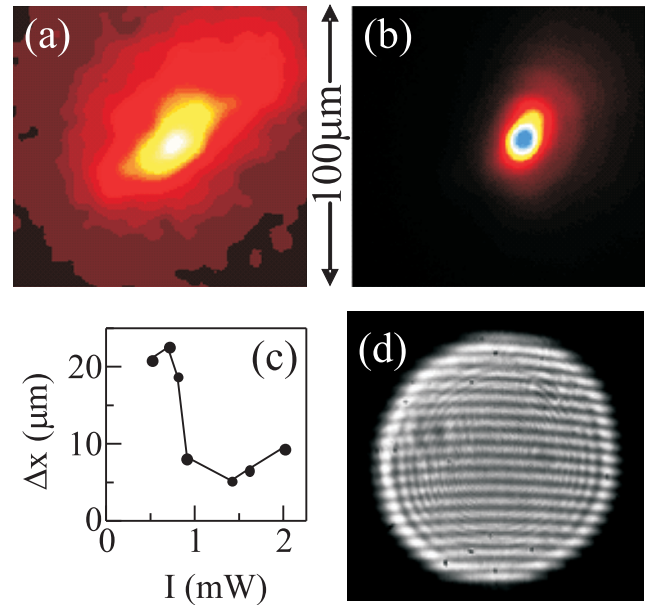

FIG. 3 (color online). Spatial distribution of polariton emission, just below (a) and just above threshold (b), and width (FWHM) of the distribution as a function of power (c). (d) k-space image of interferometrically recombined emission for time delay of 265 fs.
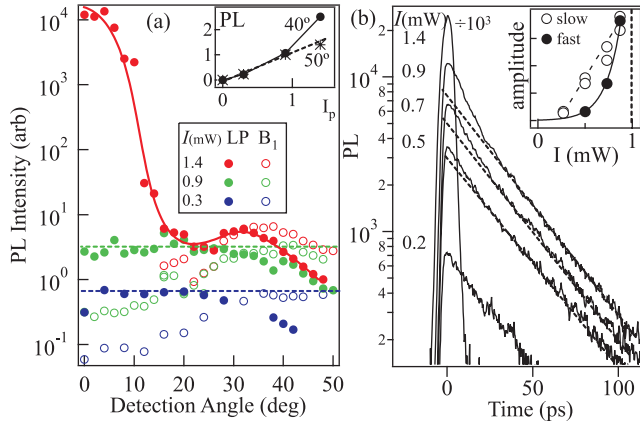
FIG. 4 (color online). (a) Extracted PL integrated intensities vs detection angle on the lower polariton branch (LP, solid points) and subsidiary Bragg mode (B_1) at three input powers, 0.3, 0.9, and 1.4 mW. Lines guide the eye at each power. (b) Time-resolved emission at normal incidence vs pump power from 0.2 mW to 1.4 mW, with amplitudes of fast and slow components extracted (inset).

passing through the threshold, as expected for polariton lasing [26]. Surprisingly, below threshold the total emission from all branches is independent of emission angle (dashed lines) and no obvious bottleneck in polariton relaxation at high k is observed in contrast to III-V and II-VI microcavities. This implies that at 300 K in GaN, phonon, exciton-exciton, and exciton-electron scattering can efficiently populate the branches giving rapid thermalization [27,28]. As the pump power is increased, the exciton population increases linearly [Fig. 4(a) inset, at 50°], while for polaritons at lower angles (e.g., 40°), the power dependence is quadratic, but suppressed in comparison to the exponentially enhanced normal emission [Fig. 2(c)].

To confirm rapid thermalization, we time resolve the buildup and decay time of the emission at normal incidence around the onset of the threshold [Fig. 4(b)] using a streak camera with 4 ps time resolution. In all cases we find an instrumentally limited rise time showing that even at low carrier densities, scattering and thermalization proceed on subpicosecond time scales. At low powers we see an exponential decay of 30 ps, attributed to trapping of excitons at nonradiative defects [29]. As the power is increased to threshold, an additional fast component rapidly rises [Fig. 4(b), dashed fits show slow decay, inset shows relative amplitudes], with decay time of 8 ps. Above threshold, the coherent emission turns on and off in <2 ps, implying that scattering from the exciton reservoir is extremely fast. The efficiency of emission increases as stimulated scattering into the lower polariton (which emits within a few ps) becomes fast in comparison to the nonradiative rates.

In conclusion, we have investigated the emission of hybrid bulk GaN microcavities at $T = 300$ K under pulsed nonresonant excitation. The observation of a low-threshold coherent emission, 1 order of magnitude smaller than in previously reported nitride-based VCSELs, and the emis-

sion line blueshift due to polariton-polariton interactions, demonstrates the first room-temperature polariton lasing.

---

*Electronic address: j.j.baumberg@soton.ac.uk

[1] *Semiconductor Microcavities*, edited by J. J. Baumberg and L. Vina [Semicond. Sci. Technol. 18, S279 (2003)].
[2] P. G. Savvidis *et al.*, Phys. Rev. Lett. **84**, 1547 (2000).
[3] R. M. Stevenson *et al.*, Phys. Rev. Lett. **85**, 3680 (2000).
[4] A. Imamoglu *et al.*, Phys. Rev. A **53**, 4250 (1996).
[5] D. Porras, C. Ciuti, J. J. Baumberg, and C. Tejedor, Phys. Rev. B **66**, 085304 (2002).
[6] G. Malpuech *et al.*, Appl. Phys. Lett. **81**, 412 (2002).
[7] H. Deng, G. Weihs, D. Snoke, J. Bloch, and Y. Yamamoto, Proc. Natl. Acad. Sci. U.S.A. **100**, 15 318 (2003).
[8] J. Kasprzak *et al.*, Nature (London) **443**, 409 (2006).
[9] M. Richard *et al.*, Phys. Rev. B **72**, 201301(R) (2005); M. Richard, J. Kasprzak, R. Romestain, R. André, and L. S. Dang, Phys. Rev. Lett. **94**, 187401 (2005).
[10] M. Saba *et al.*, Nature (London) **414**, 731 (2001).
[11] N. Antoine-Vincent *et al.*, Phys. Rev. B **68**, 153313 (2003).
[12] R. Butté *et al.*, Phys. Rev. B **73**, 033315 (2006).
[13] M. Leroux *et al.*, Phys. Rev. B **58**, R13371 (1998).
[14] G. Christmann *et al.*, Appl. Phys. Lett. **89**, 261101 (2006).
[15] J. Wagner *et al.*, J. Appl. Phys. **89**, 2779 (2001).
[16] At 300 K, the 3 different GaN excitons merge to form a single absorption line.
[17] M. Richard, R. Romestain, R. André, and L. S. Dang, Appl. Phys. Lett. **86**, 071916 (2005).
[18] From the measured 30% pump reflectivity and estimated <30% pump absorption in the GaN cavity, $N_{3D} = (1 - R)AI_p/(f_p\hbar\omega\pi r^2 L)$.
[19] F. Binet, J. Y. Duboz, J. Off, and F. Scholz, Phys. Rev. B **60**, 4715 (1999); R. A. Taylor *et al.*, Phys. Status Solidi B **216**, 465 (1999).
[20] Y.-K. Song *et al.*, Appl. Phys. Lett. **76**, 1662 (2000).
[21] Y. Yamamoto, S. Machida, and G. Björk, Phys. Rev. A **44**, 657 (1991); G. Björk, H. Heitmann, and Y. Yamamoto, Phys. Rev. A **47**, 4451 (1993).
[22] J. J. Baumberg *et al.*, Phys. Rev. B **62**, R16247 (2000).
[23] In reality, the occupation must be 1 at threshold, hence we believe the scaling of $k = 0$ density with input power is affected by uncertainty due to stimulated scattering, as well as variations in the localization of the emitting spot.
[24] P. G. Lagoudakis *et al.*, J. Appl. Phys. **95**, 8979 (2004).
[25] H. Haug and S. Koch, Phys. Status Solidi B **82**, 531 (1977).
[26] We note that this localization predicts transverse modes with a spacing $\frac{\Delta\omega}{\omega} \simeq \frac{3(\lambda_0/n)^2}{4\Delta x^2}$ of about 5 meV, in good agreement with our observations [e.g., L_{1-3}, Fig. 2(a)].
[27] P. G. Lagoudakis *et al.*, Phys. Rev. Lett. **90**, 206401 (2003).
[28] G. Malpuech, A. Kavokin, A. Di Carlo, J. J. Baumberg, Phys. Rev. B **65**, 153310 (2002).
[29] K. P. Korona, Phys. Rev. B **65**, 235312 (2002).